

Degradation mechanisms of Schottky p-GaN gate AlGaN/GaN HEMTs under high-temperature reverse bias stress

Fei Hu(胡飞), Chengbing Pan(潘成兵), Xinyuan Zheng(郑鑫源), Yibo Ning(宁一博), Xueyan Li(李雪燕), and Lixia Zhao(赵丽霞)

Citation: Chin. Phys. B, 2025, 34 (**11**): 118501. DOI: 10.1088/1674-1056/ade1c0
http://cpb.iphy.ac.cn; http://iopscience.iop.org/cpb

What follows is a list of articles you may be interested in

Recent progress on ambipolar 2D semiconductors in emergent reconfigurable electronics and optoelectronics

Yuehao Zhao(赵月豪), Haoran Sun(孙浩然), Zhe Sheng(盛喆), David Wei Zhang(张卫),Peng Zhou(周鹏), and Zengxing Zhang(张增星)

Chin. Phys. B, 2023, 32 (**12**): 128505. DOI: 10.1088/1674-1056/ad08a5

Ambipolar performance improvement of the C-shaped pocket TFET with dual metal gate and gate-drain underlap

Zi-Miao Zhao(赵梓淼), Zi-Xin Chen(陈子馨), Wei-Jing Liu(刘伟景), Nai-Yun Tang(汤乃云), Jiang-Nan Liu(刘江南), Xian-Ting Liu(刘先婷), Xuan-Lin Li(李宣霖), Xin-Fu Pan(潘信甫), Min Tang(唐敏), Qing-Hua Li(李清华), Wei Bai(白伟), and Xiao-Dong Tang(唐晓东)

Chin. Phys. B, 2023, 32 (**10**): 108502. DOI: 10.1088/1674-1056/acbaf3

Thickness effect on solar-blind photoelectric properties of ultrathin β-Ga_2O_3 films prepared by atomic layer deposition

Shao-Qing Wang(王少青), Ni-Ni Cheng(程妮妮), Hai-An Wang(王海安), Yi-Fan Jia(贾一凡), Qin Lu(陆芹), Jing Ning(宁静), Yue Hao(郝跃), Xiang-Tai Liu(刘祥泰), and Hai-Feng Chen(陈海峰)

Chin. Phys. B, 2023, 32 (**4**): 048502. DOI: 10.1088/1674-1056/ac8ce9

Dynamic electrostatic-discharge path investigation relied on different impact energies in metal-oxide-semiconductor circuits

Tian-Tian Xie(谢田田), Jun Wang(王俊), Fei-Bo Du(杜飞波), Yang Yu(郁扬), Yan-Fei Cai(蔡燕飞), Er-Yuan Feng(冯二媛), Fei Hou(侯飞), and Zhi-Wei Liu(刘志伟)

Chin. Phys. B, 2023, 32 (**4**): 048501. DOI: 10.1088/1674-1056/ac9607

DC and analog/RF performance of C-shaped pocket TFET (CSP-TFET) with fully overlapping gate

Zi-Xin Chen(陈子馨), Wei-Jing Liu(刘伟景), Jiang-Nan Liu(刘江南), Qiu-Hui Wang(王秋蕙), Xu-Guo Zhang(章徐国), Jie Xu(许洁), Qing-Hua Li(李清华), Wei Bai(白伟), and Xiao-Dong Tang(唐晓东)

Chin. Phys. B, 2022, 31 (**5**): 058501. DOI: 10.1088/1674-1056/ac43a6

Degradation mechanisms of Schottky p-GaN gate AlGaN/GaN HEMTs under high-temperature reverse bias stress

Fei Hu(胡飞), Chengbing Pan(潘成兵)[†], Xinyuan Zheng(郑鑫源), Yibo Ning(宁一博), Xueyan Li(李雪燕), and Lixia Zhao(赵丽霞)[‡]

Tianjin Key Laboratory of Intelligent Control of Electrical Equipment, School of Electrical Engineering, Tiangong University, Tianjin 300387, *China*

(Received 5 February 2025; revised manuscript received 4 June 2025; accepted manuscript online 6 June 2025)

The degradation mechanisms of Schottky p-GaN gate AlGaN/GaN HEMTs under high-temperature reverse bias (HTRB) stress were investigated and the evolution of the deep traps was identified using deep-level transient spectroscopy. The saturation current of p-GaN gate AlGaN/GaN HEMTs decreased by 18.2% and the threshold voltage shifted positively by 11.6% after the degradation. An electron trap (at 369 K) and a hole trap (at 95 K) were observed in the AlGaN/GaN region, while another hole trap (at 359 K) was found in the p-GaN layer before the stress. Meanwhile, after the stress, the concentration and capture cross section of the hole traps increased in both the p-GaN layer and the AlGaN/GaN region. With regard to the electron trap in the AlGaN/GaN region, the capture cross section increased significantly but the electron trap concentration slightly decreased, which may increase the electron trapping, thereby reducing electrons in the two-dimensional electron gas. These factors result in a positive shift in the threshold voltage and a decrease in the output current. This work provides a new insight into understanding the threshold voltage instability of Schottky p-GaN gate AlGaN/GaN HEMTs.

Keywords: semiconductor devices, III–V semiconductors, impurity, defects

PACS: 85.30.–z, 73.61.Ey, 71.55.–i

DOI: 10.1088/1674-1056/ade1c0 **CSTR:** 32038.14.CPB.ade1c0

1. Introduction

GaN-based high electron mobility transistors (HEMTs) exhibit outstanding characteristics, including high electron mobility, high breakdown electric fields, and high saturation velocity, making them highly promising candidates for high-power and high-frequency applications.[1–5] To realize normally-off GaN-based HEMTs for security operations, different methods such as the Cascode configuration,[6] recessed Schottky gate,[7] fluoride ion treatment[8] and p-GaN gate[9] have been developed. Meanwhile, due to the good thermal stability, high switching speed, and relatively lower cost, p-GaN gate technology has been widely used in commercial normally-off GaN-based HEMTs.[10,11] However, reliability issues of p-GaN gate AlGaN/GaN HEMTs have hindered their further development,[12,13] such as the threshold voltage (V_{TH}) instability, which causes the false turn-on of the circuit or gate breakdown.[14,15]

Accelerated stress tests have been used to investigate the reliability of p-GaN gate AlGaN/GaN HEMTs, among which high-temperature reverse bias stress is often employed to study the degradation behavior and failure mechanisms of AlGaN/GaN HEMTs.[16] It has been reported that the positive shift of the threshold voltage under the HTRB stress may be caused by the hole emission in the p-GaN layer.[17] In addition, the positive shift of the threshold voltage under the negative gate voltage stress can be attributed to the electron trapping in the AlGaN barrier or GaN buffer layers.[18,19] However, there are limited experimental reports regarding the defects in both the p-GaN layer and the AlGaN/GaN region of p-GaN gate AlGaN/GaN HEMTs.

In this work, we studied the degradation mechanisms of p-GaN gate AlGaN/GaN HEMTs under high-temperature reverse bias stress. To understand the degradation process of the p-GaN gate AlGaN/GaN HEMTs, we started with a low voltage of 100 V and then stepped up to 500 V at a high temperature of 200 °C. The results show that the saturation current decreased and the threshold voltage shifted positively after the stress. The concentration of the electron trap in the AlGaN/GaN region decreased slightly after the stress, while the capture cross section increased significantly. In addition, the concentration of the hole trap increased in both the p-GaN layer and the AlGaN/GaN region after the degradation. The electron trapping and the increased hole traps concentration were responsible for the positive V_{TH} shift. This work can provide a guide to understand the underlying defects in GaN-based HEMTs to address the threshold voltage instability.

2. Experimental details

In this work, the selected five devices under test (DUTs) are commercial AlGaN/GaN HEMTs with a Schottky p-GaN gate (GS66504B), which were obtained from the same production batch and exhibited identical electrical characteristics and

[†]Corresponding author. E-mail: cbpan@tiangong.edu.cn

[‡]Corresponding author. E-mail: lxzhao@tiangong.edu.cn

© 2025 Chinese Physical Society and IOP Publishing Ltd. All rights, including for text and data mining, AI training, and similar technologies, are reserved.

DLTS signals, indicating a very good consistency, as shown in Fig. S1. The HTRB stress was applied using Keithley equipments 2636B and 2657A. During the HTRB step stress, the gate–source voltage was maintained at −5 V to turn off the p-GaN gate AlGaN/GaN HEMTs, while the drain–source voltage was stepped from 100 V to 500 V (100 V, 200 V, 300 V, 400 V, 500 V), applying 9 hours at each voltage stress, to accelerate the degradation of the p-GaN gate AlGaN/GaN HEMTs and study their degradation process. The case temperature of the p-GaN gate AlGaN/GaN HEMTs was set at 200 °C during the HTRB stress.

The output and transfer characteristics were measured using a Keithley 2636B system SourceMeter instrument during the HTRB stress. Deep-level transient spectroscopy (DLTS) was measured in the temperature range from 25 K to 500 K using a Janis closed-loop helium cooling chamber and a PhyTech FT1230 HR-DLTS test system. Capacitance–voltage (*C*–*V*) curves were measured at 50 mV and 1 MHz. The thermal resistance of the p-GaN gate AlGaN/GaN HEMTs was measured using a T3Ster tester. Since the heating current should be high enough to enhance the signal-to-noise ratio of the measurement, we measured the thermal resistance using a heating current of 6 A. A focused ion beam (FIB Crossbeam 550) was employed to prepare cross-sectional transmission electron microscope (TEM) samples. Then, scanning transmission electron microscopy (Hitachi H7650) was used to compare the microstructural changes beneath the gate of the p-GaN gate AlGaN/GaN HEMTs before and after the stress.

3. Results and discussion

Figure 1(a) shows the typical output characteristics of the p-GaN gate AlGaN/GaN HEMTs at room temperature during the HTRB stress. The saturation current decreased by 18.2% from 0.99 A to 0.81 A after the degradation. Figure 1(b) shows the typical transfer characteristics of the p-GaN gate AlGaN/GaN HEMTs measured at room temperature during the HTRB stress. The transfer curve shifted to the right with the increasing stress time, and the threshold voltage increased by 0.17 V from 1.47 V to 1.64 V during the HTRB stress, as shown in the inset of Fig. 1(b).

Figure 2(a) shows that the *K* factors of the p-GaN gate AlGaN/GaN HEMTs increased by 0.05 mV/°C from 0.39 mV/°C to 0.44 mV/°C after the stress. As shown in Fig. 2(b), the thermal resistance of the chip layer increased by 0.30 K/W from 0.24 K/W to 0.54 K/W, whereas that of the die attach layer exhibited an increase of 0.73 K/W from 0.75 K/W to 1.48 K/W. The increased thermal resistance leads to an increase in the heat accumulation, which may reduce the electron mobility, resulting in a decrease in the on-state current and an increase in the on resistance.[20]

To identify potential deep levels of the p-GaN gate AlGaN/GaN HEMTs, the DLTS spectra were measured before and after the HTRB stress. Figure 3(a) shows a positive peak labeled E_1 and a negative peak labeled H_1 detected in the fresh

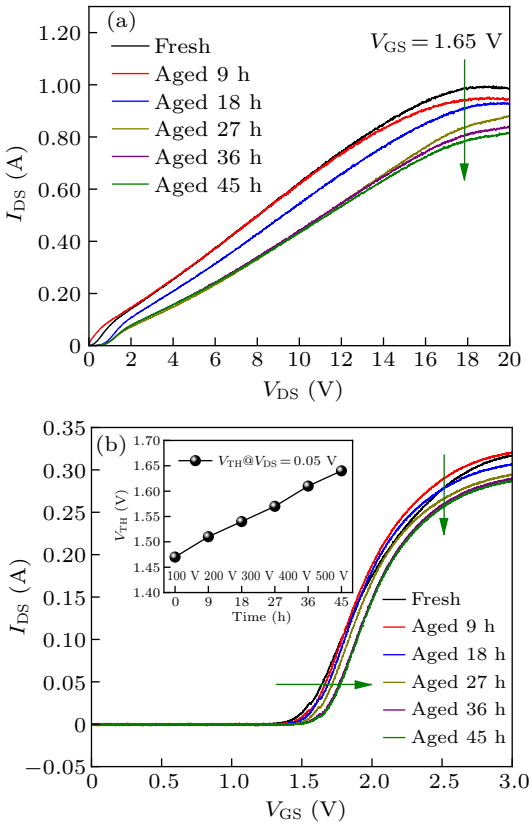


Fig. 1. (a) Output characteristics of the p-GaN gate AlGaN/GaN HEMTs during the HTRB stress. (b) Transfer characteristics of the p-GaN gate AlGaN/GaN HEMTs during the HTRB stress; the inset shows the threshold voltage of the p-GaN gate AlGaN/GaN HEMTs during the HTRB stress.

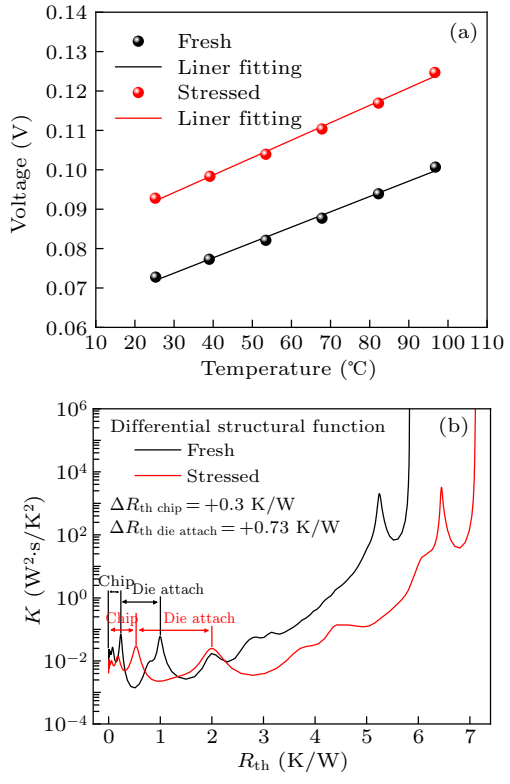


Fig. 2. (a) The *K* factors for the p-GaN gate AlGaN/GaN HEMTs before and after the HTRB stress. (b) Differential structure functions of the p-GaN gate AlGaN/GaN HEMTs before and after the degradation.

p-GaN gate AlGaN/GaN HEMTs using a bias voltage of $V_M =$ 1.2 V and a filling pulse voltage of $V_P = 2.5$ V, corresponding to the AlGaN/GaN region (Fig. S2). The temperature of the positive peak increased from 369 K to 406 K with a decrease in the peak intensity after the stress. Meanwhile, the temperature of the negative peak increased from 95 K to 104 K after the HTRB stress. In our PhyTech test system, the positive peak in the DLTS spectra is associated with majority carriers, while the negative peak corresponds to minority carriers.[21] In the AlGaN/GaN region of the p-GaN gate AlGaN/GaN HEMTs, electrons are the majority carriers and holes are the minority carriers.[22,23] For the p-GaN layer of the p-GaN gate AlGaN/GaN HEMTs, holes serve as the majority carriers and electrons are the minority carriers.

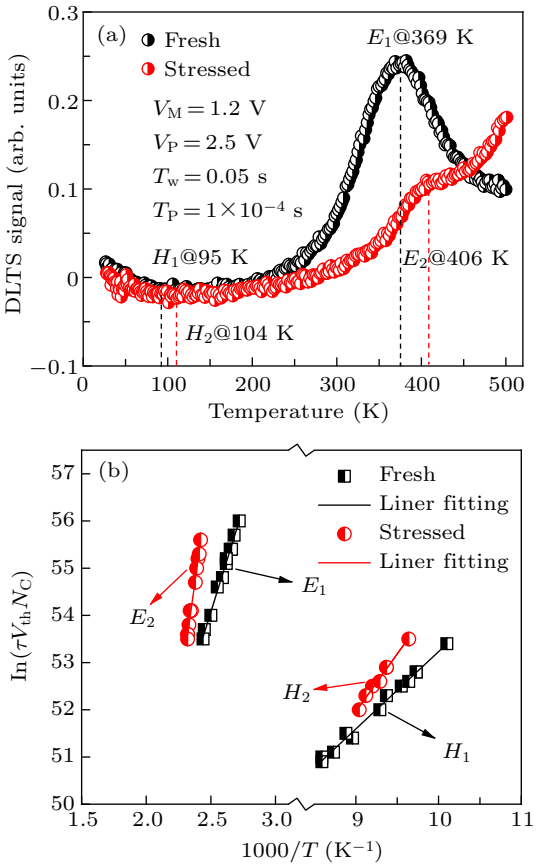


Fig. 3. (a) The DLTS spectra of the fresh and stressed p-GaN gate AlGaN/GaN HEMTs ($V_M = 1.2$ V, $V_P = 2.5$ V). (b) Arrhenius plot of the energy levels (electron traps E_1 and E_2, and hole traps H_1 and H_2) detected in DLTS.

Figure 3(b) shows the Arrhenius plots of these traps in the AlGaN/GaN region, with the calculated activation energy (E_a), trap concentration (N_T), and capture cross section (σ) of the DUT shown in Table 1. The activation energies of the electron traps E_1 and E_2 are 0.77 ± 0.02 eV and 1.64 ± 0.02 eV, respectively, with the corresponding trap concentrations of 2.01×10^{13} cm^{-3} and 1.15×10^{13} cm^{-3}, and the capture cross sections of 1.72×10^{-14} cm^2 and 7.79×10^{-5} cm^2, respectively. Moreover, the activation energies of the hole traps H_1 and H_2 are 0.14 ± 0.01 eV and 0.21 ± 0.01 eV, respectively, with the corresponding hole trap concentrations of 1.52×10^{12} cm^{-3} and 2.22×10^{12} cm^{-3}, and the capture cross sections of 9.53×10^{-17} cm^2 and 7.60×10^{-14} cm^2, respectively.

Table 1. The E_a, N_T, and σ represent the activation energy, trap concentration, and capture cross section of the traps, respectively, in the fresh and stressed p-GaN gate AlGaN/GaN HEMTs.

DUTs	Trap	E_a (eV)	N_T (cm^{-3})	σ (cm^2)
Fresh	E_1	0.77 ± 0.02	2.01×10^{13}	1.72×10^{-14}
	H_1	0.14 ± 0.01	1.52×10^{12}	9.53×10^{-17}
Stressed	E_2	1.64 ± 0.02	1.15×10^{13}	7.79×10^{-5}
	H_2	0.21 ± 0.01	2.22×10^{12}	7.60×10^{-14}

Figure 4(a) shows a positive peak labeled as H_3 at 359 K before the stress using a bias voltage of $V_M = 3$ V and a filling pulse voltage of $V_P = 5$ V, corresponding to the p-GaN layer. Meanwhile, after the stress, the positive peak shifted to a higher temperature of 368 K and increased. Figure 4(b) shows the Arrhenius plot of the hole traps in the p-GaN layer. The activation energy of the hole trap increased from 0.10 ± 0.01 eV to 0.12 ± 0.01 eV after the HTRB stress. In addition, the concentration of the hole trap increased from 4.09×10^{18} cm^{-3} to 5.80×10^{18} cm^{-3}, while the capture cross section increased from 2.40×10^{-23} cm^2 to 3.91×10^{-23} cm^2.

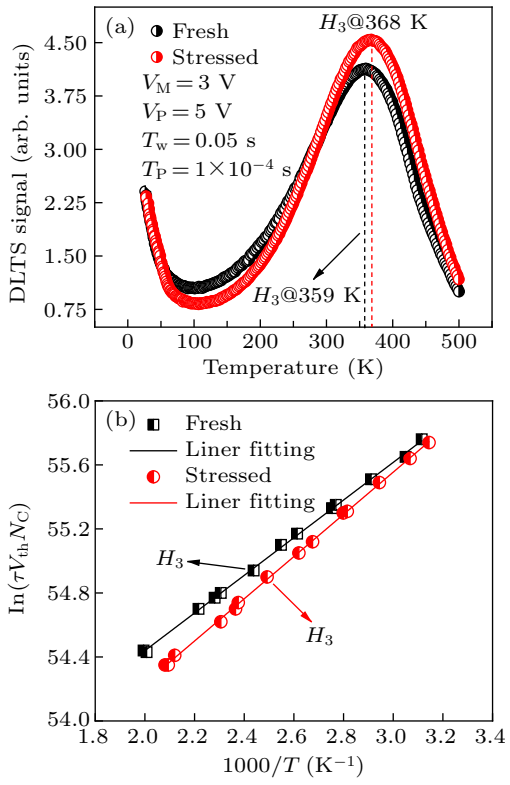


Fig. 4. (a) The DLTS spectra of the fresh and stressed p-GaN gate AlGaN/GaN HEMTs ($V_M = 3$ V, $V_P = 5$ V). (b) Arrhenius plot of the energy level hole trap H_3 detected in DLTS.

To distinguish whether the defect originated from the point defects or extended defects, the carrier trapping kinetics were also investigated. Figures 5(a) and 5(b) show the effects of filling pulse duration on the electron trap and hole trap in the AlGaN/GaN region at the peak temperature, respectively. The peak signals of the electron trap and hole trap

change linearly with the logarithm of the fill pulse width t_p. The logarithmic dependence of the DLTS peak intensity on the filling width t_p is typically observed in the traps associated with dislocations.[24–26] Figure 5(c) shows the effect of the filling pulse duration on hole traps in the p-GaN layer at the peak temperature. Before the stress, with the increasing filling pulse width, the traps represented by the DLTS signal are gradually filled, reaching a fully filled state after 10^{-4} s, indicating that the defects are related to the point defects. This is because, with the pulse width increasing, point defects are gradually filled, and subsequently the DLTS signal no longer increases once the trap is completely filled.[27] After the stress, the capture time constants of the defects may be relatively short,[28] leading to the traps being completely filled when the filling pulse duration reaches 10^{-6} s, which needs further clarification.

Figures 6(a) and 6(b) show the SEM cross-sectional images of the p-GaN gate AlGaN/GaN HEMTs prepared using a focused ion beam (FIB). STEM images of the region beneath the gate of the fresh and stressed p-GaN gate AlGaN/GaN HEMTs are shown in Figs. 6(c) and 6(d). It can be seen that after the HTRB stress, the dislocations increased in both the p-GaN layer and the AlGaN/GaN regions.

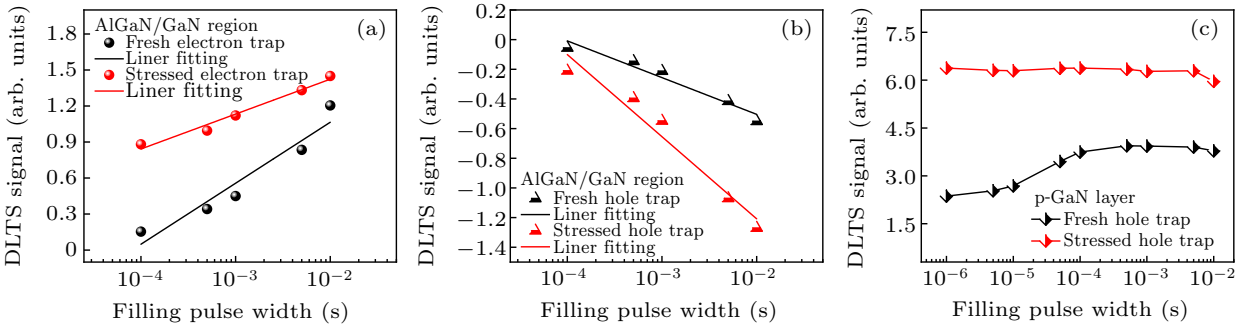


Fig. 5. The relationship between DLTS signal intensity and filling pulse width before and after the stress for (a) electron traps in the AlGaN/GaN region, (b) hole traps in the AlGaN/GaN region and (c) hole traps in the p-GaN layer of the p-GaN gate AlGaN/GaN HEMTs.

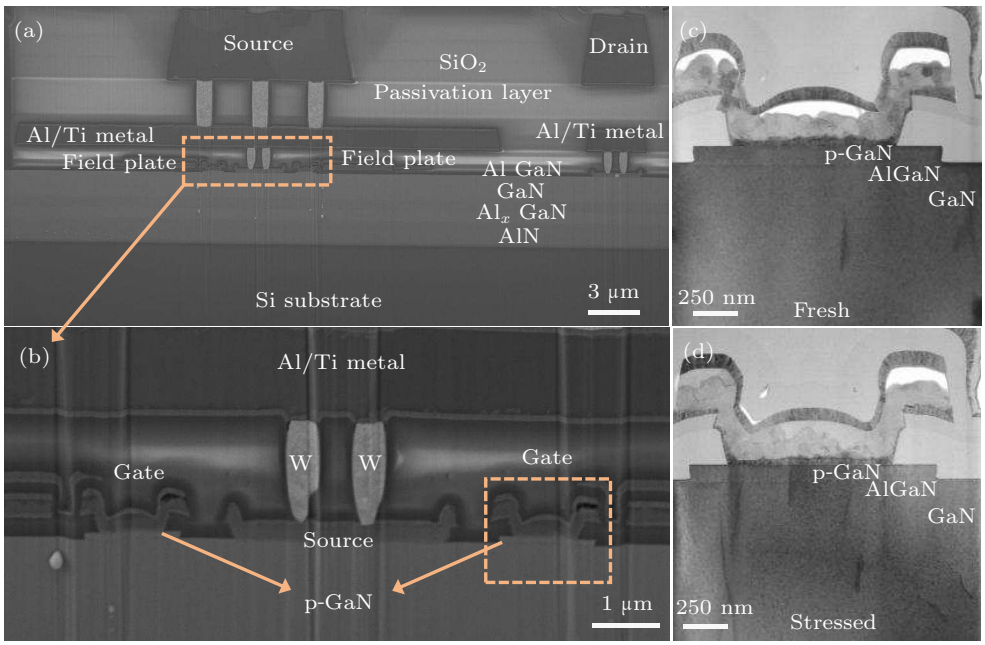


Fig. 6. (a) An SEM cross-sectional image of the fresh p-GaN gate AlGaN/GaN HEMT. (b) A zoomed SEM cross sectional image of the gate-to-source region of the fresh p-GaN gate AlGaN/GaN HEMT. (c) An STEM image of the region beneath the gate before the stress. (d) An STEM image of the region beneath the gate after the stress.

Under the HTRB stress (V_{DS} = 100 V, 200 V, 300 V, 400, 500 V, case temperature at 200 °C), a large electrical and thermal field was concentrated in the region beneath the gate,[29,30] increasing the traps in the p-GaN gate AlGaN/GaN HEMTs. The concentration of the electron trap in the AlGaN/GaN region shows a slight decrease after the stress, while the capture cross section of the electron trap increases by eight orders of magnitude, indicating increased electron trapping. The concentration and capture cross section of the hole traps in both the AlGaN/GaN region and the p-GaN layer increase. Particularly, the concentration of the hole trap in the p-GaN layer is much higher than that of the hole trap in the AlGaN/GaN region. The traps in the AlGaN/GaN region seem to be associated with the dislocations, while the trap in the p-GaN layer

is related to the point defects. The increased hole traps in the p-GaN layer would emit more holes by applying the high drain bias.[18] These factors reduce the electrons in the two-dimensional electron gas channel, resulting in the positive V_{TH} shift and the decrease in the saturation current after the stress.

Moreover, the increased concentration of the traps enhances phonon scattering,[31,32] which reduces the phonon mean free path, thereby decreasing the phonon relaxation time and propagation velocity,[33,34] and consequently decreasing the thermal conductivity and increasing the thermal resistance.[35] The increase in thermal resistance will deteriorate the heat dissipation capability of the p-GaN gate AlGaN/GaN HEMTs, which reduces the electron mobility, thereby decreasing the saturation output current.[36–38] Considering the defect changes in the p-GaN/AlGaN/GaN region after the stress, the estimated thermal resistance only increased by $\sim 30\%$.[39–41] Besides the p-GaN/AlGaN/GaN region, the traps in the AlGaN back barrier layer, AlN layer, and Si substrate may also increase after the stress and result in the thermal resistance increase in the chip, which still needs further study.

4. Conclusion

In this work, the degradation mechanisms of Schottky p-GaN gate AlGaN/GaN HEMTs were systematically investigated under high-temperature reverse bias stress. The saturation current of the p-GaN gate AlGaN/GaN HEMTs decreased by 18.2% and the threshold voltage shifted positively by 0.17 V after the degradation. The increased hole trap concentration in the p-GaN layer and the electron trapping in the AlGaN/GaN region reduce the electrons in the two-dimensional electron gas, resulting in the positive shift in the V_{TH} and the decrease in the saturation current. Moreover, the thermal resistance of both the chip and die attach increased after the HTRB stress. Our work reveals the degradation mechanisms of Schottky p-GaN gate AlGaN/GaN HEMTs under HTRB stress, and is helpful for improving the reliability of p-GaN gate AlGaN/GaN HEMTs.

Acknowledgements

Project supported by the National Natural Science Foundation of China (Grant No. 12374395) and the Chinese Institute of Electronics (CIE)-SmartChip Research Project.

References

[1] Chen L X, Ma M, Cao J C, Sun J W, Que M L and Sun Y F 2021 *Chin. Phys. B* **30** 108502
[2] Jiang X, Li C H, Yang S X, Liang J H, Lai L K, Dong Q Y, Huang W, Liu X Y and Luo W J 2023 *Chin. Phys. B* **32** 037201
[3] Zhao S L, Mi M H, Hou B, Luo J, Wang Y, Dai Y, Zhang J C, Ma X H and Hao Y 2014 *Chin. Phys. B* **23** 107303
[4] Cao Y W, Lv Q J, Yang T P, Mi T T, Wang X W, Liu W and Liu J L 2023 *Chin. Phys. B* **32** 058503
[5] Zhang Y D, Chu C S, Hang S, Zhang Y H, Zheng Q, Li Q, Bi W G and Zhang Z H 2023 *Chin. Phys. B* **32** 018509
[6] Wu Y F, Gritters J, Shen L, Smith R P, Mckay J and Barr R 2013 *The 1st IEEE Workshop on Wide Bandgap Power Devices and Applications*, October 27–29, 2013 Columbus, OH, USA, p. 6
[7] Huang S, Liu X Y, Wang X H, *et al.* 2016 *IEEE Electron Device Lett.* **37** 1617
[8] Kim Y S, Lim J Y, Seok O G and Han M K 2011 *IEEE 23rd International Symposium on Power Semiconductor Devices and ICs*, May 23–26, 2011 San Diego, CA, USA, p. 251
[9] He Y L, Zhang F, Liu K, Hong Y H, Zheng X F, Wang C, Ma X H and Hao Y 2022 *Chin. Phys. B* **31** 068501
[10] Meneghini M, Rossetto I, Rizzato V, *et al.* 2016 *Electronics* **5** 14
[11] Sayadi L, Iannaccone G, Sicre S, Häberlen O and Curatola G 2018 *IEEE Trans. Electron Devices* **65** 2454
[12] Fu K, Qi X, Fu H Q, Su P Y, Yang T H, Yang C, Montes J, Zhou J G, Ponce F A and Zhao Y J 2021 *Semicond. Sci. Technol.* **36** 014005
[13] Tallarico A N, Stoffels S, Magnone P, Posthuma N, Sangiorgi E, Decoutere S and Fiegna C 2017 *IEEE Electron Device Lett.* **38** 99
[14] Ťapajna M, Hilt O, Bahat T E, Wuerfl J and Kuzmik J 2015 *Appl. Phys. Lett.* **107** 193506
[15] Chen J T, Hua M Y, Wei J, He J B, Wang C C, Zheng Z Y and Chen K J 2021 *IEEE J. Emerg. Sel. Top. Power Electron.* **9** 3686
[16] Ionita C and Nawaz M 2017 *IEEE International Reliability Physics Symposium*, April 02–06, 2017 Monterey, CA, USA, p. WB-1.1
[17] Li S J, He Z Y, Gao R, Chen Y Q and Li C 2021 *IEEE Trans. Electron Devices* **68** 443
[18] Chao X, Tang C K, Wang C, Tan J J, Ji L, Chen L, Zhu H, Sun Q Q and Zhang D W 2022 *IEEE Trans. Electron Devices* **69** 6587
[19] Chen J T, Hua M Y, Wei J, He J B, Wang C C, Zheng Z Y and Chen K J 2021 *IEEE J. Emerg. Sel. Topics Power Electron.* **9** 3686
[20] Li X, Feng S W, Liu C, Zhang Y M, Bai K, Xiao Y X, Zheng X, He X, Pan S J, Lin G and Bai L 2020 *IEEE Trans. Electron Devices* **67** 5454
[21] Wang Y Z, Wang M S, Hua N, Chen K, He Z M, Zheng X F, Li P X, Ma X H, Guo L X and Hao Y 2022 *Chin. Phys. B* **31** 068101
[22] Tang C Y, Fu C, Jiang Y, *et al.* 2023 *Appl. Phys. Lett.* **123** 092104
[23] Das P, Halder N N, Kumar R, Jana S K, Kabi S, Borisov B, Dabiran A, Chow P and Biswas D 2014 *Electron Mater. Lett.* **10** 1087
[24] Gupta S, Simoen E, Vrielinck H, Merckling C, Vincent B, Gencarelli F, Loo R and Heyns M 2013 *ECS Trans.* **53** 251
[25] Meneghini M, Grassa M L, Vaccari S, *et al.* 2014 *Appl. Phys. Lett.* **114** 113505
[26] Venturi G, Castaldini A, Cavallini A, Meneghini M, Zanoni E, Zhu D D and Humphreys C 2014 *Appl. Phys. Lett.* **104** 211102
[27] Zheng X Y, Li H Y, Ning Y B, Pan C B, Wang K and Zhao L X 2024 *IEEE Trans. Electron Devices* **71** 6958
[28] Cho H K, Kim C S and Hong C H 2003 *J. Appl. Phys.* **94** 1458
[29] Al-Mamun N S, Islam A, Glavin N, Haque A, Wolfe D E, Ren F and Pearton S 2024 *Microelectron Reliab.* **160** 115470
[30] Romanitan C, Mihalache I, Tutunaru O and Pachiu C 2020 *J. Alloys Compd.* **858** 157723
[31] Tang D S and Cao B Y 2022 *Int. J. Heat Mass Transf.* **200** 123497
[32] Tang D S, Qin G Z, Hu M and Cao B Y 2020 *J. Appl. Phys.* **127** 035102
[33] Feng T L and Ruan X L 2014 *Journal of Nanomaterials* **2014** 206370
[34] Chatteriee B, Dundar C, Beechem T E, Heller E, Kendig D, Kim H, Donmezer N and Choi S 2020 *J. Appl. Phys.* **127** 044502
[35] Hui C X, Chen Q Q, Shi Y J, He Z Y, Huang Y, Lu X J, Wang H Y, Jiang J and Lu G G 2022 *Micromachines* **13** 2101
[36] Martinez R P, Iwamoto M, Xu J J, *et al.* 2024 *IEEE T. Microw. Theory.* **72** 2692
[37] Quay R 2008 *Gallium Nitride electronics* (Berlin: Springer-Verlag) pp. 20–25
[38] Bremer J, Chen D Y, Malko A, *et al.* 2020 *IEEE Trans. Electron Devices* **67** 1952
[39] Tang D S, Hua Y C, Zhou Y G and Cao B Y 2021 *Acta Phys. Sin.* **70** 045101 (in Chinese)
[40] Li H, Hanus R, Polanco C A, Zeidler A, Koblmuller G, Koh Y K and Lindsay L 2020 *Phys. Rev. B* **102** 104313
[41] Yang J H, Sun Y D, and Xu B 2025 *Phys. Rev. B* **111** 104112